JCTC Journal of Chemical Theory and Computation

An Accurate and Transferable Intermolecular Diatomic Hydrogen Potential for Condensed Phase Simulation

Jonathan L. Belof, Abraham C. Stern, and Brian Space*

Department of Chemistry, University of South Florida, 4202 East Fowler Avenue, CHE205, Tampa, Florida 33620-5250

Received May 7, 2008

Abstract: An anisotropic many-body H_2 potential energy function has been developed for use in heterogeneous systems. The intermolecular potential has been derived from first principles and expressed in a form that is readily transferred to exogenous systems, e.g. in modeling H_2 sorption in solid-state materials. Explicit many-body polarization effects, known to be important in simulating hydrogen at high density, are incorporated. The analytic form of the potential energy function is suitable for methods of statistical physics, such as Monte Carlo or Molecular Dynamics simulation. The model has been validated on dense supercritical hydrogen and demonstrated to reproduce the experimental data with high accuracy.

1. Introduction

The development of intermolecular H_2 potential energy functions has a long history.[1] The topic has generated renewed interest in recent years due to the increased theoretical study of hydrogen storage materials.[2] In this work, we present our own revisitation of the issue to include transferability, necessary for the practical simulation of hydrogen in heterogeneous materials as well as anisotropic many-body effects which have been shown to be important in modeling hydrogen at high density. For example, in modeling hydrogen sorption in Metal-Organic Framework materials (MOFs), a transferable potential is required that includes the ability to capture anisotropic many-body effects in a consistent, effective manner.[3,4]

To date, most hydrogen sorption studies of materials have focused on isotropic H_2 potentials[5–8] in particular that of Buch since it is easily transferable and accurately reproduces the bulk thermodynamic properties of hydrogen; in addition, it has been shown to calculate the correct uptake of hydrogen in weakly interacting materials. However, in heterogeneous environments where electrostatic quadrupole and induced dipole effects are non-negligible such an approach cannot reproduce the correct behavior: the isotropic potential includes these effects in a mean-field fashion, appropriate only for systems in which dispersion interactions dominate.

Previous anisotropic potentials[9–15] have focused on neat H_2, with the most notable being the highly accurate potential of Diep and Johnson; however, it is not clear how such specialized forms can be systematically mixed with chemically different environments without extensive reparameterization.[16] While the anisotropic potential of Darkrim and Levesque is both transferable and includes the quadrupole term, it has been shown to overestimate the attractive part of the potential and neglects induced many-body effects.[3]

Herein we apply high-level electronic structure calculations to the H_2-H_2 dimer and then fit an anisotropic functional form to the *ab initio* surface; electron correlation methods have been utilized as they have been shown to be crucial in accurately describing the relatively weak H_2-H_2 interaction.[9,10] This functional form contains quadrupole as well as electronic repulsion/dispersion terms that are transferable using the Lorentz−Berthelot mixing rules.

Several existing potentials[8,13,17] include nonadditive three-body dipole terms *via* Axilrod-Teller-Muto[18] dispersion, which are known to influence the structure of hydrogen at high density. In this work we apply a many-body polarization term to hydrogen and demonstrate improvement in the equation of state at high density. Further, explicit many-body polarization interactions have been demonstrated to be essential in modeling H_2 sorption in polar MOFs,[19] and the present polarization model is also transferable to such systems.

* Corresponding author e-mail: space@cas.usf.edu.

10.1021/ct800155q CCC: $40.75
Published on Web 07/17/2008

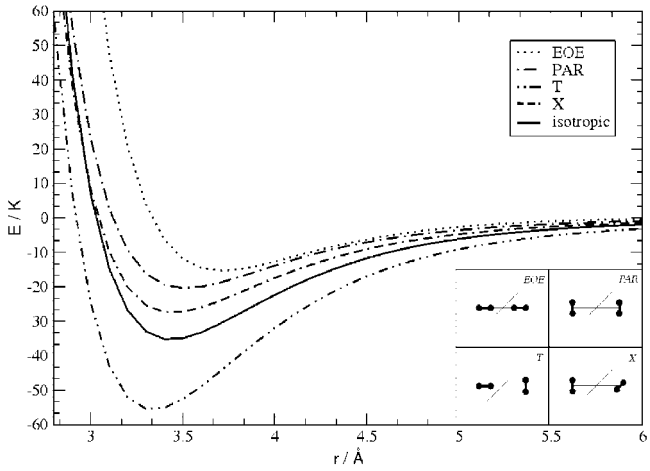

Figure 1. *Ab initio* energy curves of four distinct relative H_2 orientations (as a function of the rotor center-of-mass separation) along the Born−Oppenheimer surface. The orientations chosen were end-on-end (EOE), parallel (PAR), T-configuration (T), and X-configuration (X).

This paper is organized as follows. Section 2.1 presents the *ab initio* methods used in calculating the energy surface for the H_2-H_2 dimer. Sections 2.2 and 2.3 review the many-body polarization theory and form of the potential, respectively. Section 3 elaborates on the application of this potential toward reproducing bulk hydrogen properties. The paper is concluded in Section 4 that includes proposed applications of the transferable and highly accurate potential in predicting and retrodicting hydrogen sorption properties.

2. Methods

2.1. Born−Oppenheimer Surface. Construction of the Born−Oppenheimer surface for the H_2 dimer proceeds from optimizing the RHF[20–24] wave function parametrically as a function of the nuclear coordinates. The hydrogen molecule was approximated as a rigid rotor with a bond length of 0.742 Å, corresponding to the value determined by rotational spectra.[25,26] The surface was taken over the domain of center-of-mass separation for the rotors from 2.0 to 10.0 Å in 0.1 Å increments. A subspace of the complete surface was taken along four unique relative orientations; the orientations were chosen as being energetically and geometrically distinct (shown pictorially in Figure 1) and the four computed surfaces produce an average in agreement with experiment.[8] All electronic structure calculations were performed using the quantum chemistry code PC-GAMESS.[27,28]

Since the H_2-H_2 dimer interaction is dominated by electron correlation,[9,10] the RHF energy calculations included Møller−Plesset perturbation terms[29,30] to fourth-order,[31] including triplet states;[32] prior work in this area has sufficiently demonstrated that, for the hydrogen dimer, MP4 energies are in agreement with the CCSD(T) level of theory.[9] The set of basis functions employed in the solution of the wave function were those of Dunning[33] (aug-cc-pVTZ/QZ) with the energy eigenvalues then extrapolated to the complete basis set limit.[34] The effect of basis set superposition error was corrected by the counterpoise method.[35] The computed energy surfaces are depicted in Figure 1 along with the isotropically averaged surface.

Table 1. H_2 Molecular Polarizability Tensor (Molecular Bond Axis Aligned along the Z Axis) Calculated *via* Time-Dependent Hartree-Fock along with its Rescaled Components[a]

component	TDHF/Å^3	rescaled/Å^3
XX	0.6831	0.6945
YY	0.6831	0.6945
ZZ	0.9561	0.9720
isotropic	0.7741	0.7870

[a] The components were rescaled such that the isotropic polarizability, $^1/_3Tr\{\alpha\}$, matched experiment subject to the constraint that the ratio of TDHF values, *XX*/*ZZ*, be preserved.

The electric quadrupole value for H_2 was calculated from the electronic wave function (MP4-SDTQ/aug-cc-pVQZ) and found to be 0.664 D·Å, a value comparable to other investigations.[25,36] The molecular (static) polarizability tensor of the monomer was determined *via* TDHF[37] since it has been shown to accurately reproduce nonlinear optical properties at frequencies away from resonance; the resultant components are listed in Table 1. The components of the TDHF polarizability tensor were then rescaled such that the isotropic polarizability matched the experimental value[38] of 0.787 Å^3 subject to the constraint that the ratio of the *XX* to *ZZ* TDHF components remains invariant. Prior work has shown that, for H_2, the nonadiabatic contributions to both the quadrupole and polarizability are negligible.[36,39]

2.2. Many-Body Polarization. Here we briefly review the Thole-Applequist polarization model−details can be found elsewhere.[40–42] Briefly, the atomic point dipole, $\vec{\mu}$, of the i^{th} atom is

$$\vec{\mu}_i = \alpha_i \vec{E}_i^{stat} \tag{1}$$

where α_i is an atomic site polarizability tensor, and $\vec{E}_i^{stat}$ is the electrostatic field vector. We can decompose the dipole into separate *static* and *induced* contributions as follows

$$\vec{\mu}_i = \alpha_i^{\circ}\left(\vec{E}_i^{stat} + \vec{E}_i^{ind}\right) = \alpha_i^{\circ}\left(\vec{E}_i^{stat} - T_{ij}\vec{\mu}_i\right) \tag{2}$$

where α_i° is a *scalar* point polarizability, and T_{ij} is the dipole field tensor which, when contracted with the dipole $\vec{\mu}_j$, represents the electrostatic contribution of the j^{th} dipole toward inducing the i^{th} dipole.

The dipole field tensor is constructed based upon the positions and scalar point polarizabilities of the system and can be derived from classical electrostatic principles as

$$T_{ij}^{\alpha\beta} = \frac{\delta_{\alpha\beta}}{r_{ij}^3} - \frac{3x^{\alpha}x^{\beta}}{r_{ij}^5}$$

with an additional aspect of the model being that the second dipole may be taken to be a model distribution, with the intent that the discontinuity at short-range will be avoided; here we employ the common exponential charge distribution and associated damping parameter of 2.1304.

Equation 2 is a self-consistent field equation with respect to the dipoles and hence must be solved iteratively. However, it is possible to recast the field equations in matrix form as

$$A\vec{\mu} = \vec{E}^{\text{stat}} \tag{3}$$

where the matrix A is constructed from block matrices according to

$$A = \left[(\alpha^{\circ})^{-1} + T_{ij}\right] \tag{4}$$

The advantage to eq 4 is that the solution is then exact (to numerical precision), without the additional complication of iteration and convergence. Upon inversion of the A matrix, the molecular polarizability tensor can then be easily determined by

$$\alpha_{\alpha\beta}^{mol} = \sum_{i,j} \left(A_{ij}^{-1}\right)_{\alpha\beta} \tag{5}$$

The polarizable aspect of the hydrogen model was developed as follows. With the molecule aligned along the Z axis, the polarizability tensor was calculated with the Thole model (i.e., eq 5) and compared with the *ab initio* TDHF tensor; the scalar point polarizabilities being varied until the two tensors agree. The scalar polarizabilities, α°, were assigned at the same nuclear coordinates as the partial charges, Q, used in producing the quadrupole. The matrix in eq 4 was constructed, inverted, and then summed according to eq 5 yielding a trial polarizability tensor. The resulting trial tensor was then compared to the rescaled tensor in Table 1, and the α°'s were adjusted until the difference was minimized. The site polarizabilities were completely converged (i.e., the molecular polarizability tensor determined *via* eq 5 matched the rescaled tensor in Table 1 to within all significant digits) and are listed in Table 2.

2.3. Potential Energy Function. The interest of this work is the development of a potential energy function for use in Monte Carlo or Molecular Dynamics simulation of hydrogen interacting with heterogeneous systems. In this context, the following functional form was chosen for the potential energy function

$$U = U_{rd} + U_{es} + U_{pol} \tag{6}$$

where U_{rd} is the energy of electronic repulsion/dispersion, U_{es} is the electrostatic energy, and U_{pol} is the many-body polarization energy given by

$$U_{\text{pol}} = -\frac{1}{2}\sum_{i}^{N} \vec{\mu}_i \cdot \vec{E}_i^{\text{stat}} \tag{7}$$

where the site dipoles are found by either matrix inversion of eq 3 or iterative solution of the dipole field equations given by expression 2. For the purpose of fitting the potential energy function, we employed the matrix inversion method for maximal accuracy in the many-body potential since the computations are fast for a two-rotor system (however, in application toward condensed-phase systems the iterative method is used almost exclusively).

All of the free parameters of these functions have well-established ways of being "mixed", thereby imparting transferability. It is the main contribution of this work that these functions have been fit to the first principles data presented in Section 2.1.

Table 2. Parameter Fits for the Intermolecular Hydrogen Potential, including Many-Body Polarization Terms[a]

site	R/Å	Q/e	α°/Å^3	ε/K	σ/Å
H2GP	0.000	−0.7464	0.69380	12.76532	3.15528
H2NP	0.363	0.0000	0.00000	2.16726	2.37031
H2EP	0.371	0.3732	0.00044	0.00000	0.00000

[a] H2GP corresponds to the center-of-mass site, H2EP coincides with the true atomic locations (which, when combined with H2GP, provides the quadrupole), while H2NP contains the additional Lennard-Jones sites.

The electrostatic energy follows from the quadrupole-quadrupole interactions between the hydrogen monomers. Given the quadrupole value of 0.664 D·Å calculated from first principles and a bond length of 0.742 Å, this corresponds to partial charges of $Q = +0.3732e$ at the atomic sites and $-2Q$ at the center-of-mass.

The short-range electronic repulsion and long-range dispersion energies are included in U_{rd} by use of the Lennard-Jones 12−6 potential function. Since the Lennard-Jones r^{-6} part includes a mean-field long-range polarization, it was necessary that U_{rd} be determined. With U_{es} and U_{pol} functionally held fixed, U_{rd} was varied *via* simulated annealing such that $(U\text{-}U_{BO})^2$ was minimized (where U_{BO} is the Born−Oppenheimer energy surface found in Section 2.1). The results of the potential energy function fitting are shown in Figure 2. Given the anisotropic nature of the Born−Oppenheimer potential demonstrated in Figure 1, Figure 2 demonstrates that our relatively simple and transferable potential can capture the essential anisotropy. Interestingly, while the T orientation shows the largest deviation from the *ab initio* surface, even dramatically increasing the number of Lennard-Jones parameters did not significantly improve the fit. Note, given the large variation in the potential it is critical in modeling hydrogen in highly anisotropic environments that the potential capture these structural characteristics.

In the course of the parameter-space search, the Lennard-Jones sites on the hydrogen molecule were allowed to move off their nuclear centers. In addition, searches were made that constrained the sites to be both on and off the bond axis, with as few as two and as many as nine simultaneous sites in an attempt to improve the fit; it was found, however, that three sites constrained to the bond axis were optimal in terms of having the minimized error (with only marginal improvement in the fit upon increasing the number of sites further). At the end of the fitting process, the parameters that minimized the error were found and are presented in Table 2. In order to also develop a nonpolarizable potential, the process was repeated with $U_{pol} = 0$. In physical systems where the magnitude of electrostatic polarization is negligible, the nonpolarizable parameters presented in Table 3 are desirable for the reduced computational cost.

3. Model Validation

3.1. Second Virial Coefficient. Quantum mechanical corrections to the second virial coefficient of a gas can be systematically derived using the Wigner-Kirkwood distribution function.[43] To order h^4, we have the semiclassical series

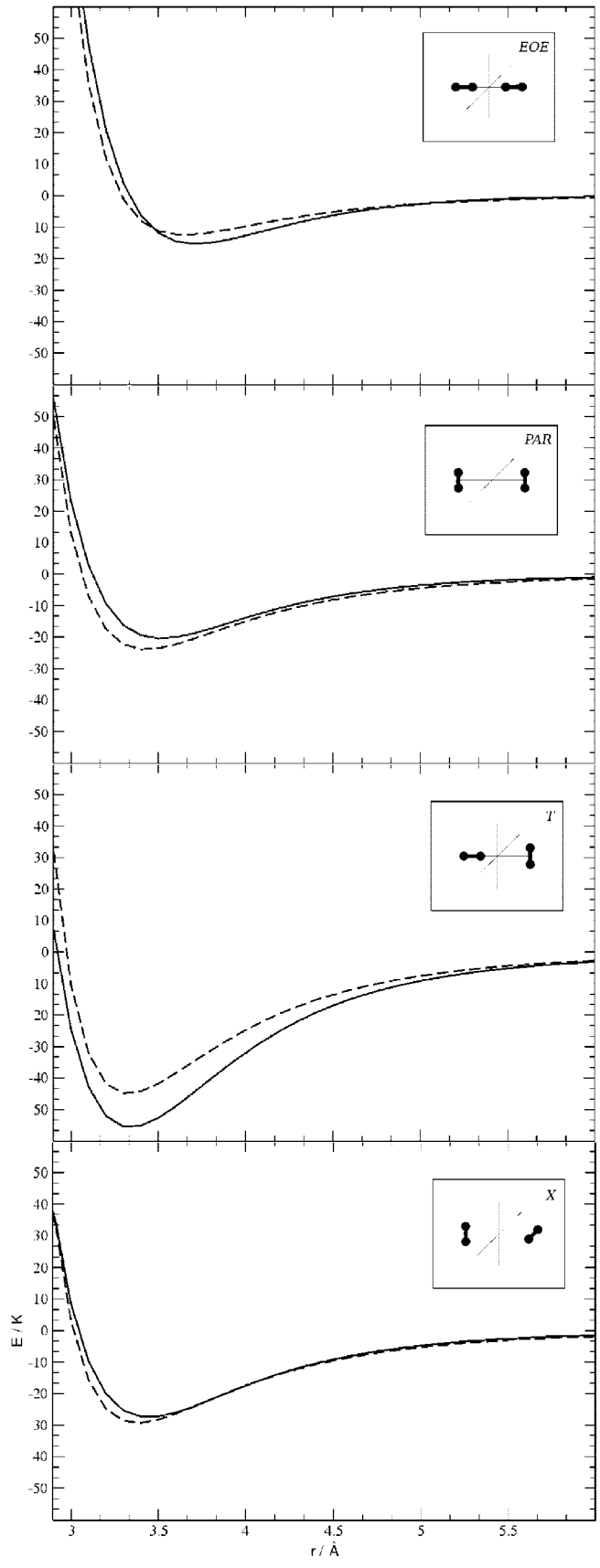

Figure 2. Potential energy curves found by fitting to eq 6 (dashed) versus the *ab initio* curves from Figure 1 (solid). The alternative nonpolar form ($U_{pol} = 0$) that was also fit to the *ab initio* data is not shown for clarity since, with a slight exception to the T configuration, the curves are visually indistinguishable.

Table 3. Potential Parameters for the Pairwise Model (Neglecting Polarization Terms)

site	R/Å	Q/e	ε/K	σ/Å
H2G	0.000	−0.7464	8.8516	3.2293
H2N	0.329	0.0000	4.0659	2.3406
H2E	0.371	0.3732	0.0000	0.0000

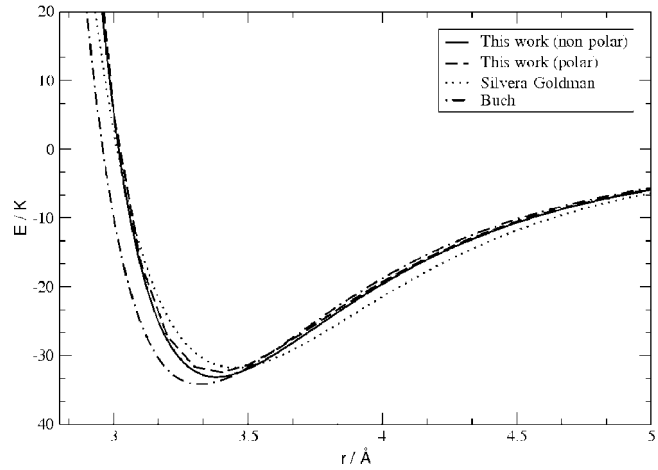

Figure 3. The isotropic projection $\phi(r)$ of the many-body potential U is shown along with the SG and Buch potentials.

$$B_2(T) = 2\pi\int_0^\infty dr\, r^2(1-e^{-\beta\varphi}) + \frac{h^2}{24\pi\beta^3}\int_0^\infty dr\, r^2 e^{-\beta\varphi}\left[\frac{\partial\varphi}{\partial r}\right]^2 + \frac{h^4}{960\pi^3\beta^4}\int_0^\infty dr\, r^2 e^{-\beta\varphi}\times\left\{\left[\frac{\partial^2\varphi}{\partial r^2}\right]^2 + \frac{2}{r^2}\left[\frac{\partial\varphi}{\partial r}\right]^2 + \frac{10\beta}{9r}\left[\frac{\partial\varphi}{\partial r}\right]^3 - \frac{5\beta^2}{36}\left[\frac{\partial\varphi}{\partial r}\right]^4\right\} \quad (8)$$

where $\phi(r)$ is an isotropic potential as a function of the separation. The intermolecular many-body potential developed here has been spherically averaged to produce an isotropic pair potential, $\phi(r)$, which is plotted in Figure 3 along with the well-known isotropic potentials of Silvera-Goldman[8] and Buch,[7] both of which are known to closely match experiment.

The second virial coefficient, $B_2(T)$, was then calculated *via* eq 8. Numerical integration was performed for r = 0.001−25 Å across a temperature range spanning from 50 to 500 K, in 10 K increments. The results are compared with experiment[38] (and the SG potential) in Figure 4.

3.2. Equation of State. The equation of state was ascertained by calculating the average number of hydrogen molecules, $\bar{N}$, via sampling of the grand canonical ensemble for a corresponding range of chemical potential. The following statistical mechanical expression was numerically estimated by Grand Canonical Monte Carlo[44,45]

$$\bar{N} = \frac{1}{\Xi}\sum_{N=0}^{\infty} e^{\beta\mu N}\left\{\prod_{i=1}^{3N}\int_{-\infty}^{\infty} dx_i\right\} N e^{-\beta U(x_1,\ldots,x_{3N})}$$

where the chemical potential of the gas reservoir, μ, was determined through empirical fugacity functions[46,47] for

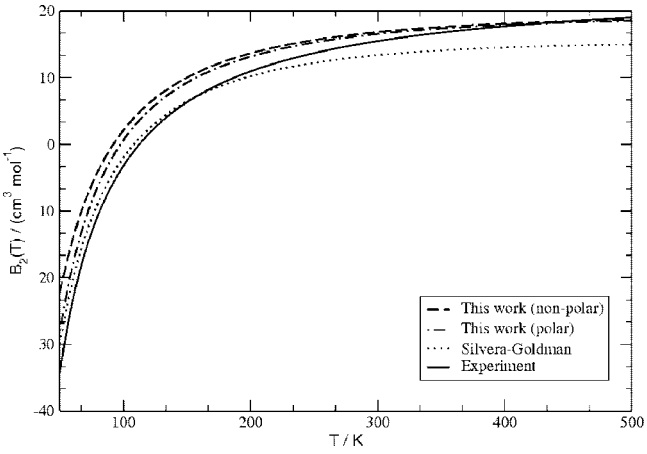

Figure 4. $B_2(T)$ from 50−500 K for the polarizable and nonpolarizable potentials including Wigner-Kirkwood quantum corrections to order $\hbar^4$.

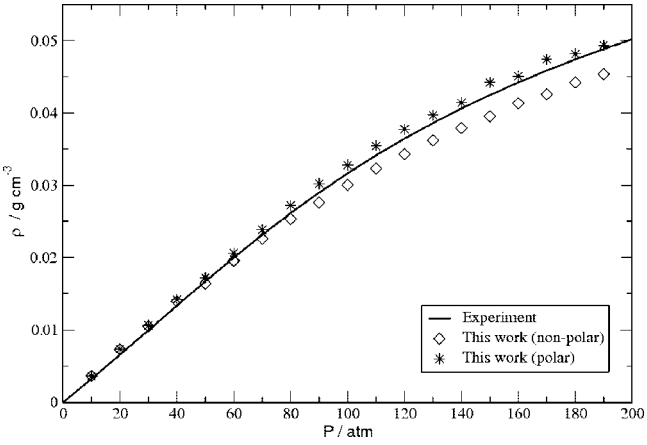

Figure 5. P-ρ plot of hydrogen at 77 K using the first principles-derived potential energy function. The densities were calculated using GCMC over the corresponding pressure range, including empirical fugacity corrections. The electronic repulsion/dispersion energy term included Feynman-Hibbs quantum effects to order $\hbar^4$; the data generated without this correction were systematically higher by about 10%. All data points have a maximum variance of ±0.001 g cm $^{-3}$.

hydrogen at both high and low temperature (the high-pressure densities have also been verified *via* NPT molecular dynamics). Isothermal P-ρ curves were generated at temperatures of 77 K (pressure range of 0−200 atm) and 298.15 K (pressure range of 0−2000 atm), and the results are compared with experimental data[48,49] in Figures 5 and 6. For the simulations at 77 K, Feynman-Hibbs quantum corrections[50] were applied to the energetically dominant electronic repulsion/dispersion part of the potential to order $\hbar^4$ *via*

$$U_{rd}^{FH} = U_{rd} + \frac{\beta\hbar^2}{24\mu}\left(U_{rd}'' + \frac{2}{r}U_{rd}'\right) + \frac{\beta^2\hbar^4}{1152\mu^2}\left(\frac{15}{r^3}U_{rd}' + \frac{4}{r}U_{rd}''' + U_{rd}''''\right) \quad (9)$$

where U_{rd}', U_{rd}'',... are the derivatives of the electronic repulsion/dispersion term of eq 6 with respect to the displacement r. These corrections were not applied in the generation of the 298.15 K data since these effects are negligible at room temperature. To reduce the computational cost, these quantum corrections were only applied to the repulsion/dispersion energy because at 77 K, under the pressure conditions demonstrated here, the repulsion/dispersion energy is greater than 85% of the total energy.

It should be pointed out that the molecular hydrogen is in a supercritical phase under the conditions reported. Note the liquid hydrogen density at boiling (20 K) is 0.07 g cm $^{-3}$; thus the state points considered include those representative of relatively strong intermolecular interactions for H_2. In both instances, we see improved agreement with experiment at high-density when many-body effects are explicitly considered by inclusion of U_{pol}. It is known that many-body polarization effects are of even greater importance when considering high-density hydrogen interacting strongly with, for example, a polar adsorbing material.[4]

4. Conclusions

An anisotropic, many-body hydrogen potential has been derived from first principles and expressed in a functional form suitable for mixing with heterogeneous systems consisting of partial charges, Lennard-Jones sites, and atomic point polarizabilities. It has been shown to reproduce the properties of bulk hydrogen under conditions of current interest in materials research. Electrostatic quadrupolar and many-body polarization interactions are included anisotropically, thus making this model useful for high-density studies where orientation-dependence is of interest.

Next, it is planned to use the potential in modeling H_2 sorption in highly polar MOFs that have been shown to sorb hydrogen at near liquid densities at 77 K.[4,19] The potential should also be useful in modeling hydrogen in any condensed phase system where the essential physics of the composite system is captured by the flexible potential energy function presented.

Acknowledgment. Computations were performed on the Ranger supercomputer located at the Texas Advanced Computing Center under a Teragrid Grant (Grant No. TG-CHE070098N) and also at the USF Research Computing Center. The authors acknowledge funding from the Depart-

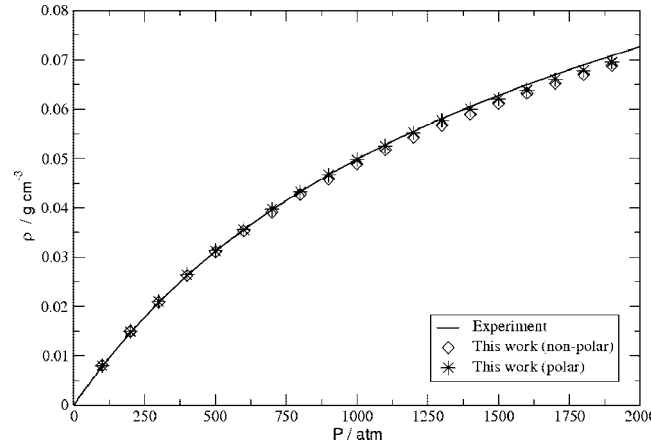

Figure 6. P-ρ plot of hydrogen at 298.15 K using the first principles-derived potential energy function. All data points have a maximum variance of ±0.0008 g cm $^{-3}$.

ment of Energy (Grant No. DE0GG02-07ER46470) and the National Science Foundation (Grant No. CHE-0312834). The authors also thank the Space Foundation (Basic and Applied Research) for partial support.

References

(1) Van Kranendonk, J. *Solid Hydrogen: Theory of the Properties of Solid H_2, HD, and D_2*, 2nd ed.; Plenum Press: New York, 1983; p 45.

(2) Long, J. R.; Alivisatos, A. P.; Cohen, M. L.; Frechet, J. M. J.; Head-Gordon, M.; Louie, S. G.; Zettl, A.; Richardson, T. J.; Mao, S. S.; Read, C.; Alkire, J. A Synergistic Approach to the Development of New Classes of Hydrogen Storage Materials, 2005;Department of Energy Hydrogen Program. http://www.hydrogen.energy.gov (accessed Mar 3, 2008).

(3) Garberoglio, G.; Skoulidas, A. I.; Johnson, J. K. *J. Phys. Chem. B* **2005**, *109*, 13094.

(4) Belof, J.; Stern, A.; Eddaoudi, M.; Space, B. *J. Am. Chem. Soc.* **2007**, *129*, 15202.

(5) Schaefer, J.; Watts, R. *Mol. Phys.* **1982**, *47*, 933.

(6) Knaap, H.; Beenakker, J. *Physica* **1961**, *27*, 523.

(7) Buch, V. *J. Chem. Phys.* **1994**, *100*, 7610.

(8) Silvera, I. F.; Goldman, V. V. *J. Chem. Phys.* **1978**, *69*, 4209.

(9) Diep, P.; Johnson, J. K. *J. Chem. Phys.* **2000**, *112*, 4465.

(10) Diep, P.; Johnson, J. K. *J. Chem. Phys.* **2000**, *113*, 3480.

(11) Gallup, G. *Mol. Phys.* **1977**, *33*, 943.

(12) Etters, R.; Danilowicz, R.; England, W. *Phys. Rev. A* **1975**, *12*, 2199.

(13) Wind, P.; Røeggen, I. *Chem. Phys.* **1996**, *211*, 179.

(14) Mulder, F.; van der Avoird, A.; Wormer, P. *Mol. Phys.* **1979**, *37*, 157.

(15) Darkrim, F.; Levesque, D. *J. Chem. Phys.* **1998**, *109*, 4981.

(16) Zhang, Z.; Duan, Z. *J. Chem. Phys.* **2005**, *122*, 214507.

(17) Kostov, M. K.; Cole, M. W.; Lewis, J. C.; Diep, P.; Johnson, J. K. *Chem. Phys. Lett.* **2000**, *332*, 26.

(18) Axilrod, B.; Teller, E. *J. Chem. Phys.* **1943**, *11*, 299.

(19) Liu, Y.; Eubank, J.; Cairns, A.; Eckert, J.; Kravtsov, V.; Luebke, R.; Eddaoudi, M. *Angew. Chem., Int. Ed.* **2007**, *46*, 1433.

(20) Hartree, D. *Proc. Camb. Phil. Soc.* **1928**, *24*, 89.

(21) Fock, V. *Z. Phys. A* **1930**, *62*, 795.

(22) Slater, J. *Phys. Rev.* **1932**, *42*, 33.

(23) Slater, J. *Phys. Rev.* **1950**, *81*, 385.

(24) Roothaan, C. *Rev. Mod. Phys.* **1951**, *23*, 69.

(25) Johnson, R. D. NIST Computational Chemistry Comparison and Benchmark Database. http://srdata.nist.gov/cccbdb (accessed Mar 3, 2008).

(26) Herzberg, G. *Molecular Spectra and Molecular Structure*, 2nd ed.; Krieger Publishing Co.: Malabar, FL, 1989; Vol. I, p 532.

(27) Nemukhin, A. V.; Grigorenko, B. L.; Granovsky, A. A. *Moscow University Chem. Bull.* **2004**, *45*, 75.

(28) Schmidt, M. W.; Baldridge, K. K.; Boatz, J. A.; Elbert, S. T.; Gordon, M. S.; Jensen, J. J.; Koseki, S.; Matsunaga, N.; Nguyen, K. A.; Su, S.; Windus, T. L.; Dupuis, M.; Montgomery, J. A. *J. Comput. Chem.* **1993**, *14*, 1347.

(29) Møller, C.; Plesset, M. S. *Phys. Rev.* **1934**, *46*, 618.

(30) Binkley, J.; Pople, J. *Int. J. Quantum Chem.* **1975**, *9*, 229.

(31) Krishnan, R.; Pople, J. *Int. J. Quantum Chem.* **1978**, *14*, 91.

(32) Krishnan, R.; Pople, J. *J. Chem. Phys.* **1980**, *72*, 4244.

(33) T.H. Dunning, J. *J. Chem. Phys.* **1989**, *90*, 1007.

(34) Helgaker, T.; Klopper, W.; Koch, H.; Noga, J. *J. Chem. Phys.* **1997**, *106*, 9639.

(35) Boys, S.; Bernardi, F. *Mol. Phys.* **1970**, *19*, 553.

(36) Poll, J.; Wolniewicz, L. *J. Chem. Phys.* **1978**, *68*, 3053.

(37) Karna, S.; Dupuis, M. *J. Comput. Chem.* **1991**, *12*, 487.

(38) Lide, D. R. *Handbook of Chemistry and Physics*, 84th ed.; CRC Press: Boca Raton, FL, 2003.

(39) Kolos, W.; Wolniewicz, L. *J. Chem. Phys.* **1967**, *46*, 1426.

(40) Bode, K. A.; Applequist, J. *J. Phys. Chem.* **1996**, *100*, 17820.

(41) Thole, B. *Chem. Phys.* **1981**, *59*, 341.

(42) van Duijnen, P. T.; Swart, M. *J. Phys. Chem. A* **1998**, 102, 2399.

(43) Brack, M.; Bhaduri, R. K. *Semiclassical Physics*; Westview Press: Boulder, CO, 2003; p 148.

(44) Metropolis, N.; Rosenbluth, A. W.; Rosenbluth, M. N.; Teller, A. H.; Teller, E. *Phys. Lett. B* **1953**, *21*, 1087.

(45) Frenkel, D.; Smit, B. *Understanding Molecular Simulation: From Algorithms to Applications*, 2nd ed.; Academic Press: New York, 2002; p 129.

(46) Shaw, H.; Wones, D. *Am. J. Sci.* **1964**, *262*, 918.

(47) Zhou, L.; Zhou, Y. *Int. J. Hydrogen Energy* **2001**, *26*, 597.

(48) Lemmon, E.; McLinden, M.; Friend, D. NIST Chemistry WebBook. Linstrom, P., Mallard, W., Eds. http://webbook.nist.gov (accessed Mar 5, 2008).

(49) Younglove, B. *J. Phys. Chem. Ref. Data* **1982**, *11*, 1.

(50) Feynman, R.; Hibbs, A. *Quantum Mechanics and Path Integrals*; McGraw-Hill: New York, 1965; p 281.

CT800155Q